Lecture 8

Elemental Imaging of Mouse ES Cells

8.1. Introduction

Embryonic stem (ES) cells are expected to bring the breakthrough in the therapy for progressive neurodegenerative disorders such as Parkinson's disease, Alzheimer's disease and Huntington disease [1-3]. ES cells are generally called pluripotent stem cell and are unique in that they have the capacity for unlimited self-renewal along with the ability to produce multiple different types of terminally differentiated descendants as shown in figure 8.1 [2]. The differentiation of ES cells can be controlled in vitro by choosing the configuration of culture conditions. The in vitro differentiation of mouse ES cell has been widely investigated and several methods to produce cardimyocytes, hematopoietic stem cells and endothelial cells are established [4-6]. To utilize ES cells for the therapy of neurodegenerative disorders, it is necessary to establish the method to culture dopaminergic neurons in vitro. The conditions required for neural cell induction had been unknown for a long time, but recently two groups identified their own methods using mouse ES cells [7, 8].

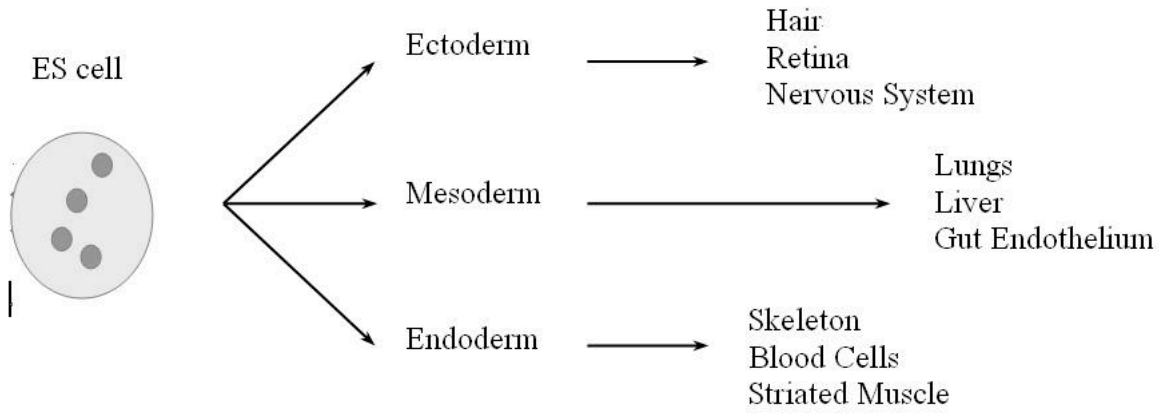

Figure 8.1. Schematic drawing of pluripotency of mouse embryonic stem (ES) cells. ES cells are unique in that they have the capacity for unlimited self-renewal along with the ability to produce multiple different types of terminally differentiated descendants.

McKay et al. cultured dopaminergic and serotonergic neurons in the presence of mitogen and specific signaling molecules and generated neuronal cells [9]. Another group lead by Sasai identified the substance that is generated from PA6 stromal cells and promotes neural differentiation of mouse ES cells. They named this substance stromal cell-derived inducing activity (SDIA) [10].

Although the procedure to induce neuronal differentiation is partially revealed, the details of the mechanism are unknown. Therefore it remains quite difficult to culture neurons efficiently for therapeutic application. Recently there are several genetic studies to elucidate the mechanism of differentiation and organogenesis [11-14].

In this study, a new approach was taken to investigate the mechanism of differentiation by dissecting the change of distributions, concentrations and chemical states of intracellular trace elements. It is considered that trace metal elements and metalloproteins are deeply related to the orientation of differentiation as active centers as well as the neural cell death in neurodegenerative disorders [15].

The aim of this study is to analyze the distribution, concentration and chemical states of the trace elements in the process of differentiation of mouse ES cells, and to understand how they can be related to the differentiation. The investigations of the differentiation have never been carried out from the aspect of these elemental conditions at the cell level. From the experimental results, the unelucidated points, e.g., i) how the intracellular elements change in the process of the neuronal differentiation and ii) the optimal elemental conditions for neuronal differentiation are considered. The information obtained in this study will be valuable from the viewpoint of not only the neuroscience but also basic biology about development of nervous system and evolution [16].

In this study, x-ray fluorescence (XRF) and x-ray near edge structure (XANES) analysis were applied to understand the multiple elemental conditions in different stages of differentiation efficiently and at the high sensitivity. Mouse ES cells form the colonies in the process of cell culture and each colony is in the different states of differentiation. Conventional chemical analysis methods enable simple quantification, but the information that is specific to each colony is lost in these methods because they require the fragmentation and solution of samples. XRF and XANES analysis does not require any

pretreatments of samples to analyze the trace elements. These techniques are also nondestructive so it is possible to observe the progress of differentiation or the generation of neurotransmitters such as dopamine histochemically by immunostaining after the elemental analysis to the same samples. These features are a significant advantage that can not be obtained in other techniques for studying the differentiation of mouse ES cells.

The study in this chapter can be divided into two experimental parts. In the first part of the study, the effect of differentiation to the intracellular trace elements was investigated. The change in the concentrations and proportions of intracellular elements were investigated in the process of acquiring various functions and differentiating. The specific orientation of differentiation such as the neuronal induction was not performed in this experiment. After that, the neuronal differentiation was induced by the SDIA method that was suggested by Sasai et al. and the mechanism of neuronal development was considered. The chemical states of the transitional metal elements (Fe and Zn) are analyzed by XAFS technique in addition to elemental concentrations and distributions.

8.2. Investigation about the Effect of the Uunoriented Differentiation

8.2.1. Cell Culture and Sample Preparation

Two groups first derived mouse ES cells from mouse embryos in 1981 [17,18]. Culturing ES cells technique is well established and now it is the essential technique for the transfection and producing transgenic mice [1, 19]. Mouse ES cells are isolated from the inner cell mass (ICM) of postconception mouse blastocysts. To maintain the pluripotency of the mouse ES cells, they have to be cocultured with feeder layers of inactivated mouse primary embryonic fibroblasts. A feeder cell layer of fibroblasts prevents the differentiation of ES cells and makes them proliferate in undifferentiated states. The main aim of this study, however, is to consider the effect of the progress of the differentiation to the elemental distributions and concentrations. Therefore the feeder layer of fibroblasts were omitted to promote the differentiation into a variety of cell types and elicit the effect of differentiation.

The mouse ES cells (129/Sv) were purchased from Cell & Molecular Technologies, Inc. and the passage number (the age of cell line) was 15 in the beginning of the cell culture. The differentiation proceeds according to the increase of the passage number. The optical microscopic photographs of the cultured mouse ES cells whose passage numbers were 15, 16 and 17 are shown in figure 8.2.

Figure 8.2 (a) shows the cells at the time of initial plating to gelatin-treated dishes and the passage number was 15. It can be seen that the cells adhered to the bottom of the culture dish isolatedly. After 3 days the cells formed colonies as seen in (b). Once the dishes are crowded and the colonies are large, the colonies are detached from the dish with Trypsin/EDTA, broken up into single cells and passaged into other gelatin-coated dishes. Figure 8.2 (c) and (d) shows the photographs at the passage number 16 and 17 respectively. The morphological change of the ES cells of getting flat and dark can be observed in accordance with the repeated passages and it is the typical characteristic of the progress of the differentiation.

Samples for the elemental analysis were prepared by fixing colonies that had been cultured on Mylar films with 20 % formalin solution. Three and two samples are made at the passage number 16 and 17. These samples are referred as 16-1, 16-2, 16-3, 17-1 and 17-2 respectively. The second numbers shows the period of sample preparation and larger number means longer period of cell culture.

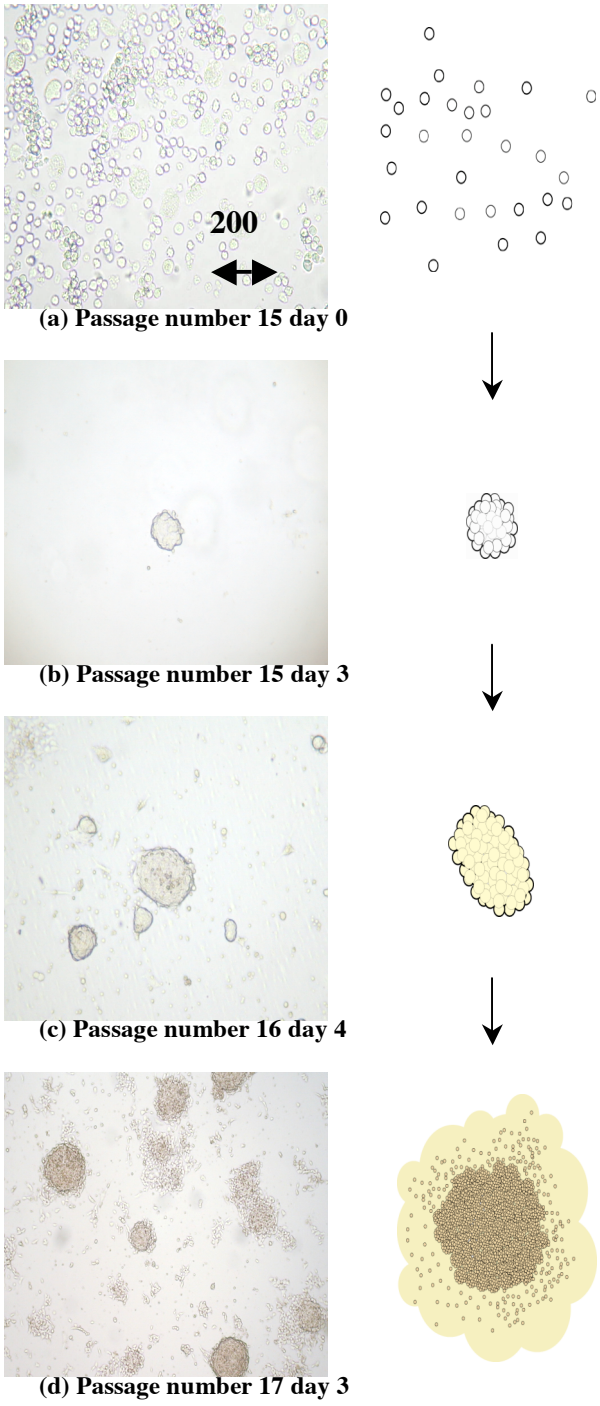

Figure 8.2. The optical microscopic photographs of the cultured mouse ES cells whose passage numbers were (a and b) 15, (c) 16 and (d) 17. The morphological change of getting flat and dark can be observed in accordance with the repeated passages and it is the typical future of the progress of the differentiation

8.2.2. XRF Analysis and Results

The SR-XRF analyses in this investigation were performed at Photon Factory in beam line 4A. The incident x-ray energy was 14.3 keV and the beam size was approximately 7 × 5 μm^2. The detailed set-up of the beam line is described in chapter 2. The analyses were carried out in air.

The elemental distribution images were obtained in the three or four areas that contained colonies in each sample. The typical elemental images of (b) P, (c) S, (d) Cl, (e) Fe and (f) Zn and the corresponding (a) microscopic photographs of the samples at the passage number 16 and 17 are shown in figure 8.3 and 8.4, respectively. The scale on the right side of the images shows the count of the x-ray intensity. Red and blue pixels show areas of high and low intensities respectively. The measurement areas were 99 × 99 μm^2 for figure 8.3 and 144 × 144 μm^2 for figure 8.4, and the measurement time was both 6 sec/point. The range of intensity was from 0 to 41 for P, 0 to 44 for S, 14 to 146 for Cl, 17 to 290 for Fe and 6 to 29 for Zn in figure 8.3 and from 0 to 98 for P, 0 to 90 for S, 1 to 22 for Cl, 0 to 23 for Fe and 2 to 51 for Zn in figure 8.4 respectively. From the results of the imaging, the measurement points were selected for further quantitative point-measurement. XRF spectra were obtained at these points to reveal the distribution ratios among elements. The measurement time was 200 seconds. The typical spectra that were obtained in the colonies at the passage number 16 and 17 are shown as solid lines in figure 8.5 (a) and (b) respectively with the spectra obtained outside of the colonies shown as dotted lines. Each spectrum is normalized with the incident x-ray intensity. The spectra obtained in the colonies shown in figure 8.5 (a) and (b) are compared in figure 8.6. The solid and dotted spectra show those obtained at the passage number 16 and 17 respectively. Quantitative analysis was then applied to all measured spectra and the calculated values for concentrations of S, P, Cl, Fe and Zn are shown in table 8.1. The thickness and the density of the colonies are considered as 50 μm and 1.0 g/cm^3 respectively.

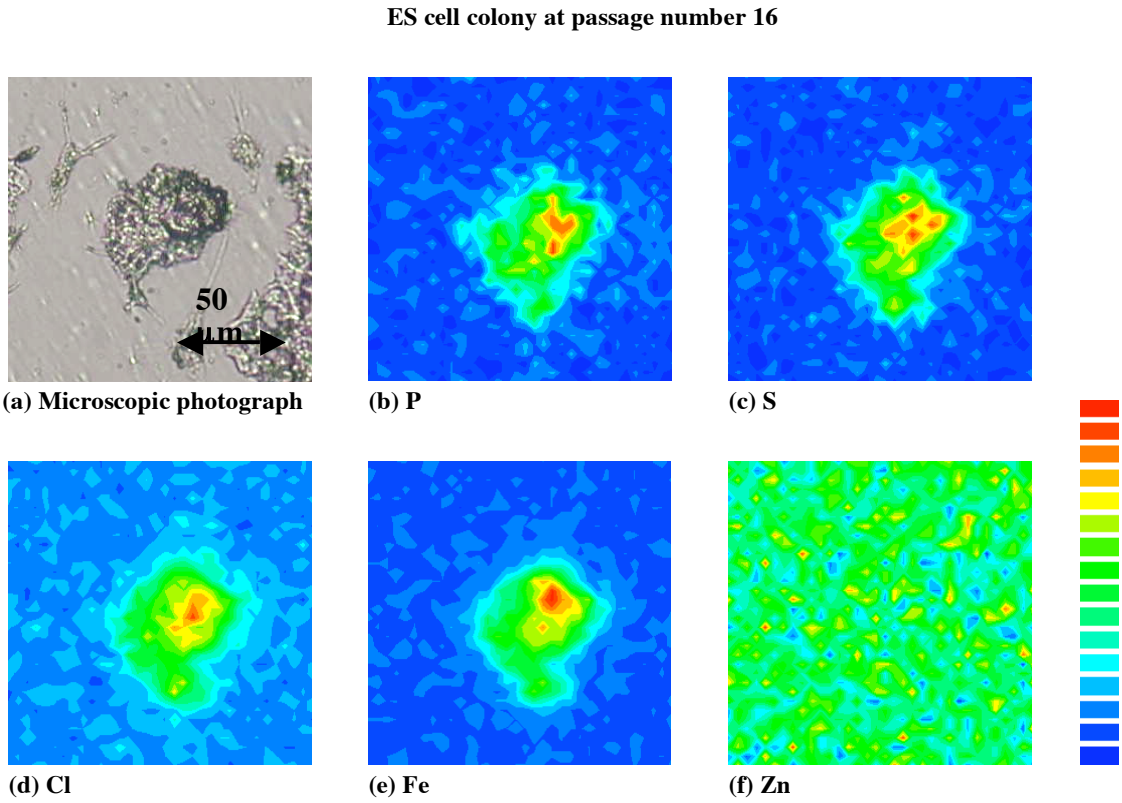

Figure 8.3. The typical elemental images of (b) P, (c) S, (d) Cl, (e) Fe and (f) Zn obtained in the mouse ES cell colony at passage number 16 shown in (a) microscopic photograph. The colony contained intracellular P, S, Cl and Fe but the concentration of Zn was low.

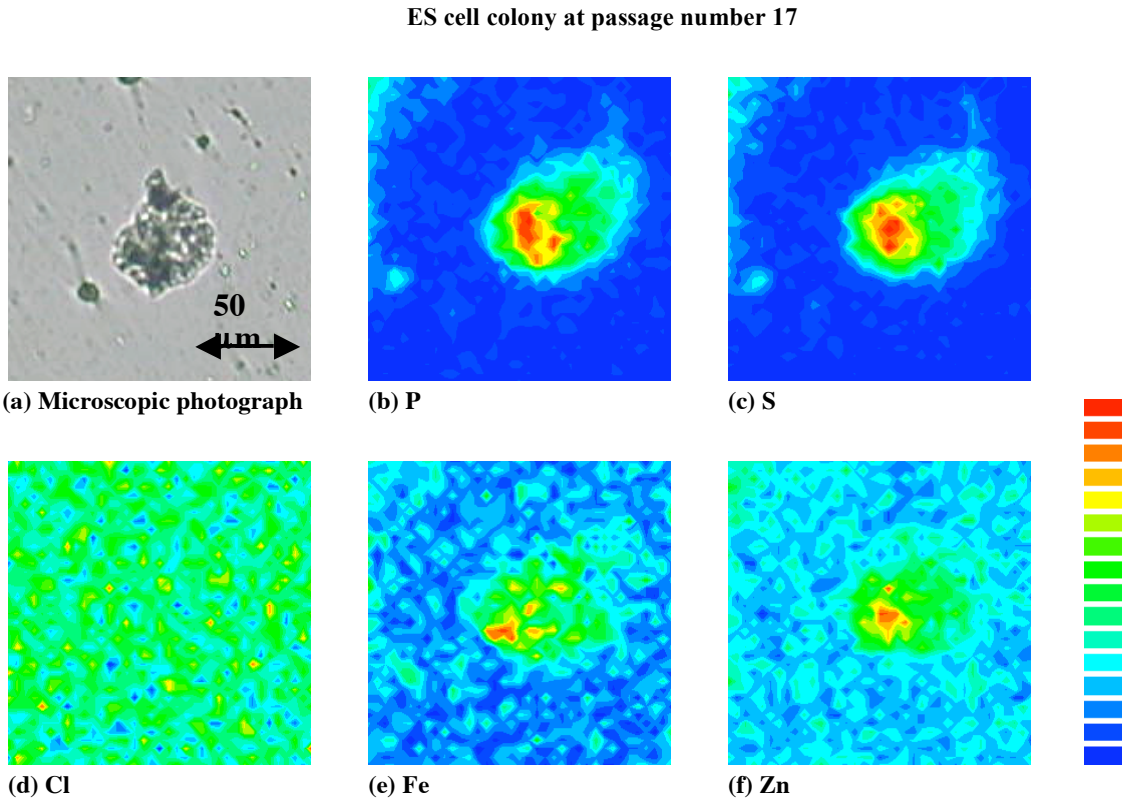

Figure 8.4. The typical elemental images of (b) P, (c) S, (d) Cl, (e) Fe and (f) Zn obtained in the mouse ES cell colony at passage number 17 shown in (a) microscopic photograph. The colony contained P, S, Fe and Zn. The distribution of Cl could not be measured due to the low concentration while Zn was low in the colony at passage number 16.

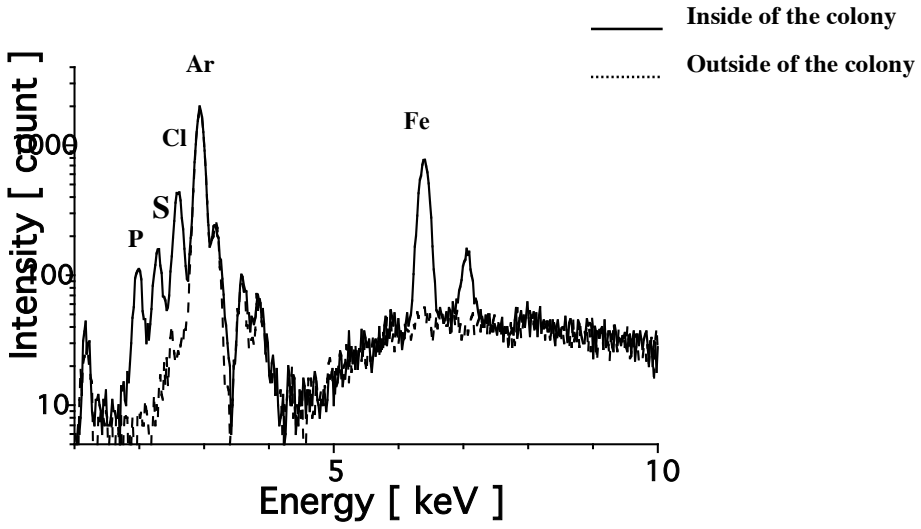

(a) The typical spectrum obtained in the mouse ES cell colony of the passage number 16

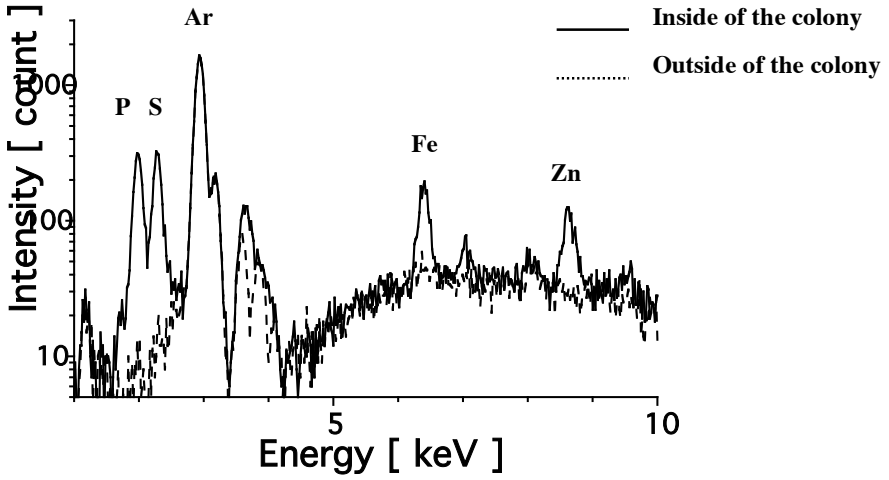

(b) The typical spectrum obtained in the mouse ES cell colony of the passage number 17

Figure 8.5. The typical XRF spectra obtained in the mouse ES cell colonies at the passage number (a) 16 and (b) 17. The solid and dotted spectra show those obtained inside and outside of the colonies respectively. It was confirmed that the elements such as P, S, Cl, Fe and Zn were contained in the colonies not in the culture medium

8.2.3. Discussion

In figure 8.3, it can be seen that the colony whose passage number is 16 contained (b) P, (c) S, (d) Cl and (e) Fe while the distribution of (f) Zn could not be detected at a considerable level due to the low concentration. The distributions of (b) P, (c) S, (d) Cl and (e) Fe were almost identical. This result indicates that these elements are contained in this colony uniformly and suggests that the cells in this colony are in the same stage of differentiation. In figure 8.4, the fluorescent x-ray intensity from (f) Zn was high and that of (d) Cl was low in the colony whose passage number is 17 though it contained (b) P, (c) S and (e) Fe. The concentration of Cl had decreased and that of Zn had increased according to the progress of differentiation. And the distributions of Fe and Zn are slightly different from those of P and S. This fact suggests that the cells in this colony had differentiated into several different cell types.

From the XRF spectra shown in figure 8.5 (a) and (b), it was confirmed that these colonies contained the elements P, S, Cl, Fe and Zn. The peaks of Ar in these spectra were due to Ar contents in the air. Figure 8.6 shows the comparison of the typical spectra the passage number 16 (solid line) and 17 (dotted line). It can be seen that the height of the peak of Cl is low and that of Zn is high in the passage number 17. This is supportive for the results of the elemental imaging.

To confirm this difference, the quantification results from each colony were compared. The absolute area densities of the intracellular elements are not so important because the sizes of the colonies were different from each other (approximately 60 – 200 μm in the diameter). In the present study, the relative ratios of each element to phosphorus are compared. The intracellular content of phosphorous has been considered as the index of intracellular organic content because it is a constituent of nondiffusible solutes that carries a net negative charge [20]. Figure 8.7 (a), (b) and (c) shows the relative amounts of S, Cl and Zn to phosphorus in the samples respectively. The values of S/P (figure 8.7 (a)) are similar in all samples. But the values of Cl/P (b) had distinctly decreased and those of Zn/P (c) had increased in accordance with the increase of the passage number from 16 to 17.

Zn plays a key role in genetic expression, cell division, and growth in several ways and is essential for function of many enzymes [21, 22]. Mouse ES cells differentiate into a variety of cell types and the proliferation is activated as the passage is repeated. It is probable that the increase of Zn is deeply related to the growth and acquisition of cell functions. Furthermore the transcription factors with zinc-finger DNA-binding domains such as GATA-1 are required for the regulation of the differentiation into specific cells [23]. It is also possible that these transcription factors had increased in mouse ES cells, as the directions of differentiation were determined in each colony.

Cl ions are mostly known to participate in the modulation of cell excitability. The Cl gradient across cell membranes adjusts the membrane potential and it is also related to the regulation of intracellular pH and cell volume [24]. There is the possibility that these parameters had changed due to the progress of differentiation and/or the activation of cells, and the change had resulted in the decrease of Cl. In order to elucidate the effect of the change in chloride concentration, other analyses techniques should be applied complementarily for the in vivo measurement of the membrane potential or intracellular pH.

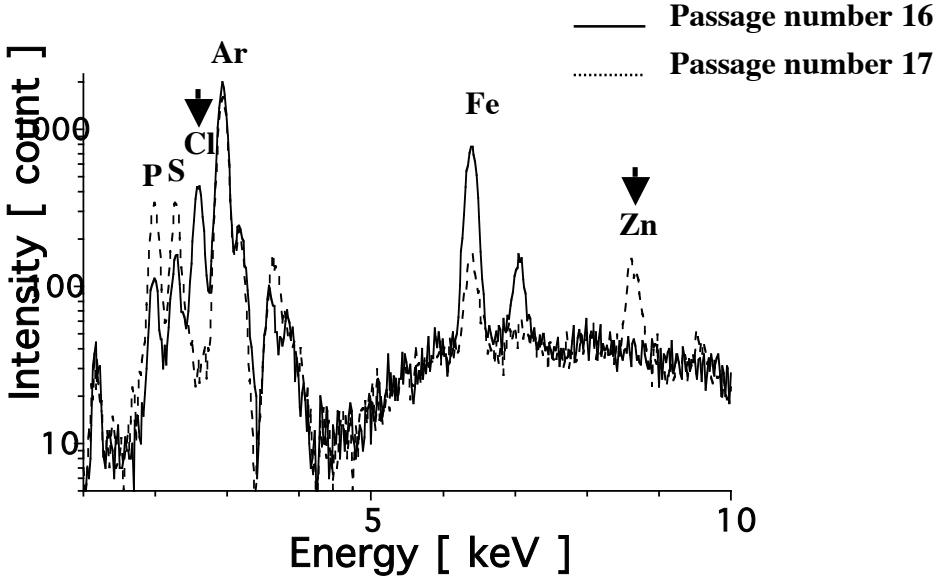

Figure 8.6. The comparison of the typical XRF spectra obtained in the mouse ES cell colonies at the passage number 16 (solid line) and 17 (dotted line). It is suggested that chlorine had decreased and zinc had increased according to the progress of differentiation.

Table 8.1. The quantification results obtained by processing XRF spectra with the computer program that was introduced in chapter 2. The concentrations of P, S, Cl, Fe and Zn in the mouse ES cell colonies were quantified and shown in ppm.

		P	S	Cl	Fe	Zn
16-1	colony 1	1121.2± 283.6	657.0± 188.4	651.1± 145.5	67.2± 77.4	3.4± 1.1
	2	1150.2± 307.5	713.9± 201.3	318.2± 76.9	32.1± 24.3	8.7± 3.0
	3	1119.7± 169.5	685.4± 90.3	461.5± 28.1	32.4± 34.6	8.2± 3.7
	4	1373.4±1862.7	692.6± 764.0	746.5± 777.2	49.7± 55.5	2.9± 0.9
16-2	1	499.8± 161.9	411.8± 175.0	940.5± 278.0	199.3± 71.4	3.0± 0.8
	2	1960.2± 461.6	1445.8± 415.8	917.4± 204.6	981.6±266.8	5.4± 1.3
	3	1401.4± 399.9	1129.9± 274.1	944.7± 211.3	714.5±140.2	4.5± 1.5
	4	925.2± 99.6	695.3± 120.5	744.5± 54.2	426.5± 38.8	4.6± 2.1
16-3	1	1774.1± 864.3	1087.9± 126.2	920.3± 92.3	64.5± 61.7	12.6± 7.4
	2	3421.±2240.5	2266.5±1277.6	1637.4± 686.4	110.5± 61.4	37.2±18.5
	3	2666.5±1726.6	1840.6±1027.0	1731.9± 921.0	94.2± 47.6	40.4±19.2
	4	272.2± 72.6	194.5± 57.4	247.1± 45.1	28.9± 5.5	3.0± 0.2
17-1	1	1633.4± 825.9	1055.9± 328.8	61.1± 5.7	52.0± 18.4	17.4± 7.1
	2	393.9± 170.0	277.0± 110.8	61.2± 12.1	24.6± 12.9	3.6± 1.1
	3	1165.4± 967.4	772.0± 630.5	54.1± 10.6	24.7± 11.7	13.7±10.5
17-2	1	1409.3± 782.4	884.6± 506.2	295.1± 111.7	53.7± 33.2	8.1± 5.5
	2	1986.2± 654.6	1158.0± 316.3	476.3± 131.5	79.3± 55.5	9.3± 6.4
	3	2489.2± 669.1	1544.8± 433.1	259.6± 71.6	68.6±106.1	23.3±13.3

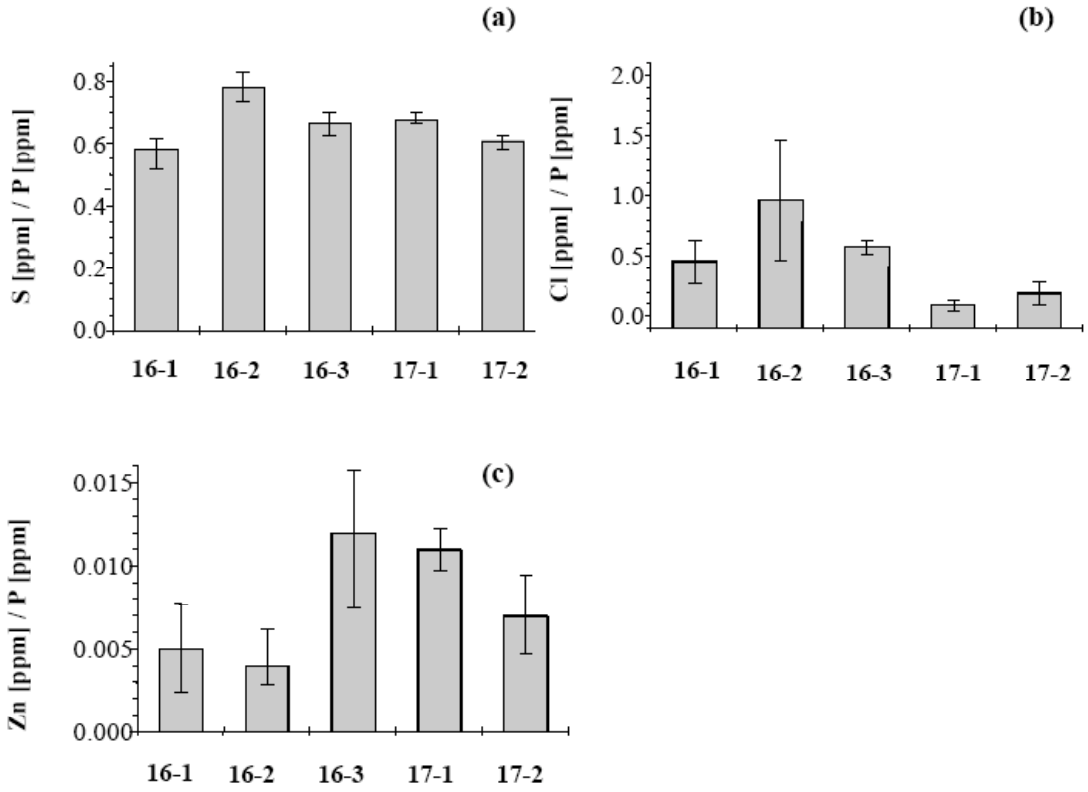

Figure 8.7. The relative amounts of (a) S, (b) Cl and (c) Zn to phosphorus respectively in the sample 16-1, 2, 3, 17-1 and 2. The values of S/P (a) are almost similar in all samples. But the values of Cl/P and Zn/P distinctly had changed in accordance with the increase of the passage number from 16 to 17.

References

1. S. Gokhan, M.F. Mehler, *Anat. Rec.,* **2001**, 265, 142.
2. M. Hynes, A. Rosenthal, *Neuron,* **2000**, 28, 11.
3. S.B. Dunnett, A. Bjorklund, O. Lindvall, *Nature Rev. Neurosci.,* **2001**, 2, 365.
4. M.G. Klug, M.H. Soonpaa, G.Y. Koh, L.J. Field, *J. Clin. Invest.,* **1996**, 98, 216.
5. M. Kennedy, M. Firpo, K. Chol, C. Wall, S. Robertson, N. Kabrun, G. Keller, *Nature*, **1997**, 386, 488.
6. G. Keller, M. Kennedy, T. Papayannopoulou, M.V. Wiles, *Mol. Cell. Biol.,* **1993**, 13, 473.
7. J.A. Robertson, *Nature Rev. Genet.,* **2001**, 2, 74.
8. A. Fraichard, O. Chassande, G. Bilbaut, C. Dehay, P. Savatier, J. Samarut, *J. Cell Sci.,* **1995**, 108, 3181.
9. S.H. Lee, N. Lumelsky, L. Studer, J.M. Auerbach, R.D. McKay, *Nature Biotech.,* **2000**, 18, 675.
10. H. Kawasaki, K. Mizuseki, S. Nishikawa, S. Kaneko, Y. Kuwana, S. Nakanishi, S. Nishikawa, Y. Sasai, *Neuron*, **2000**, 28, 31.
11. M. Lako, S. Lindsay, J. Lincoln, P.M. Cairns, L. Armstrong, N. Hole, *Mech. Dev.,* **2001**, 103, 49.
12. J.F. Loring, J.G. Porter, J. Seilhamer, M.R. Kaser, R. Wesselschmidt, *Restor. Neurol. Neurosci.,* **2001**, 18, 81.
13. A. Streit, A.J. Berliner, C. Papanayotou, A. Sirulnik, C.D. Stern, *Nature,* **2000**, 406, 74.
14. V. Tropepe, S. Hitoshi, C. Sirard, T.W. Mak, J. Rossant, D. Van der Kooy, *Neuron*, **2001**, 30, 65.
15. L.A. Hanna, J.M. Peters, L.M. Wiley, M.S. Clegg, C.L. Keen, *Toxicol.*, **1997**, 116, 123.
16. K.S. O'Shea, *Anat. Rec.,* **1999**, 257, 32.
17. M.J. Evans, M.H. Kaufman, *Nature,* **1981**, 292, 154.
18. G.R. Martin, *Proc. Natl. Acad. Sci. USA,* **1981**, 78, 7634.
19. "*Animal Cell Electroporation and Electrofusion Protocols*", *Methods in molecular biology*, vol. 48, ed. J.A. Nickoloff, Humana Press, **1995**, 167.

20. S. Larsson, A. Aperia, C. Lechene, *Am. J. Physiol.,* **1986**, 251, C455.
21. H.H. Sandstead, *J. Lab. Clin. Med.,* **1994**, 124, 322.
22. R.S. MacDonald, *J. Nutr.,* **2000**, 130, 1500S.
23. L. Pevny, M.C. Simon, E. Robertson, W.H. Klein, S.F. Tsai, V.D. Agati, S.H. Orkin, F. Constantini, *Nature,* **1991**, 349, 257.
24. L. Garcia, M. Rigoulet, D. Georgescauld, B. Dufy, P. Sartor, *FEBS Lett.,* **1997**, 400, 113.